NASA Technical Memorandum 78658

Acoustic Measurements of a Large Cavity in a Wind Tunnel

James Scheiman

MAY 1978

NASA

NASA Technical Memorandum 78658

Acoustic Measurements of a Large Cavity in a Wind Tunnel

James Scheiman
Langley Research Center
Hampton, Virginia

National Aeronautics
and Space Administration

**Scientific and Technical
Information Office**

1978

SUMMARY

Acoustic measurements of a large scale cavity have been made with inside and far-field microphones. Correlation of measured frequencies with available theories indicates that existing theories are applicable over a broader range than previously shown. A qualitative evaluation of cavity radiation efficiency indicates that acoustic radiation varies with speed and mode number. The cavity configuration with a partial covering downstream seems to amplify the tonal intensities. The frequency of the tones seems to depend on cavity size, not on cavity open area. Introducing upstream disturbances seems to decrease the amplitude of the cavity tones.

INTRODUCTION

Airframe noise is an important environmental noise problem (ref. 1). The Federal Aviation Administration (FAA) now requires all newly certified aircraft to comply with specified noise regulations. Compliance necessitates the experimental and analytical study of various sources contributing to the overall aircraft noise and of possible noise reduction techniques. One of the major airframe noise sources has been identified as the landing gear and cavity system (refs. 1 and 2). Other studies of cavity noise (refs. 3 to 17) have identified various acoustic mode shapes and radiating frequencies.

This study investigates the applicability of available theories for cavities of a larger, more realistic size. The measured radiating frequencies of a large cavity are compared with frequencies derived from available theories. The internal and external pressures are compared to evaluate the radiation efficiencies. Upstream disturbances and partially covered cavities were investigated together with a simulated landing gear.

SYMBOLS

Measurements are given in the U.S. Customary Units and the International System of Units (SI). Measurements were made in U.S. Customary Units.

c	speed of sound, m/sec (ft/sec)
D	cavity depth dimension (see table I(d) and ref. 15), m (ft)
f	acoustic cavity frequency (see table I(d) and ref. 15), Hz
f_m	acoustic cavity frequency (see table I(c) and ref. 10), Hz
f_n	acoustic cavity frequency (see table I(d) and ref. 11), Hz

K_v	constant, 0.57 (see table I(c) and ref. 10)
L	cavity length dimension (see table I(c) and ref. 10), m (ft)
M	Mach number, V/c
m, n	mode number 1, 2, 3, . . .
V	velocity over cavity, m/sec (ft/sec)
X,Y,Z	coordinate axis system
x,y,z	velocity survey coordinates (see fig. 3), m (ft)
α	constant 0.25 (see table I(c) and ref. 10)

MODELS, TEST PROGRAM, AND DATA ACQUISITION

Models

A simple, large plywood cavity was constructed for acoustic testing. The cavity was rectangular with a movable downstream vertical wall and a false bottom. This design permitted the testing of various combinations of cavity lengths and depths. The cavity width was held constant at 43.18 cm (17 in.). In order to maintain a thin boundary-layer flow over the cavity, the cavity was elevated about 0.3048 m (1 ft) above the wind-tunnel floor and was surrounded with a false floor. The leading edge of the false floor was blunted in an attempt to minimize the leading-edge noise of the false floor. A photograph of the cavity, false floor, and wind-tunnel floor is shown in figure 1. Figure 1 shows that the movable downstream vertical cavity wall was supported by a surface parallel to the floor; this parallel surface protruded slightly above the false floor.

The dimensions of the various cavity configurations tested are presented in figure 2. In addition to the variations in cavity length-to-depth ratio, numerous other configurations were tested. For example, cavity configurations G to N (fig. 2) are partially covered cavities. For configurations G and H, a partial covering was placed over the upstream end of the cavity. For configurations I and J, the covering was placed over the downstream end.

The boundary-layer thickness has been shown to affect noise radiation. (See, for example, refs. 14 and 16.) To evaluate this factor further, exaggerated upstream disturbances were installed on configurations K to N.

To evaluate the possible effect of the landing-gear strut location, configurations P and Q were included. These configurations were constructed by fastening a board to the upstream or downstream vertical walls of the cavity to simulate a landing-gear strut.

Test Program

The acoustic tests were conducted in the Langley V/STOL tunnel, which is an atmospheric closed-circuit wind tunnel. The test section measures 4.42 m (14.50 ft) high and 6.63 m (21.75 ft) wide. The test section ceiling and walls can be raised to provide an open test section. To decrease reverberation effects, the tests were conducted in the open test section; this procedure placed the ceiling 7.97 m (25.15 ft) above the tunnel floor. The tunnel wind speed was varied from 0 to a maximum of 68.6 m/sec (225 ft/sec) in intervals of 7.6 m/sec (25 ft/sec). All configurations were tested over the entire speed range except configurations L to Q which were not tested at the 68.6-m/sec (225-ft/sec) speed. As part of the test program, a flow survey was made with a probe of pitot-static tubes (rake) at various points over the false floor. Acoustic tests were repeated with the cavity completely closed (configuration A) in order to estimate the background noise. For each test point, the acoustic data were recorded after the wind speed was stabilized.

Data Acquisition

The five acoustic sensors were standard 1.27-cm (0.50-in.) Bruel and Kjaer condenser microphones. A sketch of the cavity model and the coordinates of the microphone positions are given in figure 3. Microphones 1 and 2 were located relatively close to the cavity as shown in figure 3 (at a distance of about 1.30 m (4.28 ft)) and were in the flow stream. These two microphones were fitted with a standard Bruel and Kjaer protective nose cone and were supported by a cylindrical pipe 5.556 cm (2.312 in.) in diameter. Microphones 3 and 5 were located outside of the flow stream at a distance of 8.57 m (28.11 ft) and 7.04 m (23.10 ft), respectively. (See table of coordinates in fig. 3.) Microphones 3 and 5 were located within the test chamber surrounding the test section (i.e., outside of the wind stream) and were fitted with standard Bruel and Kjaer "Nerf balls" to minimize low gust velocity noise. Microphone 4 was located flush with the forward inside vertical surface of the cavity wall.

The acoustic sensors were connected with standard preamplifiers, a power supply, and amplifiers to a recording system which was a 14-channel FM tape recorder. Calibrations were performed before and after each series of tests to verify the stability of the overall amplitude and frequency response of the measurement system and the data reduction system.

A velocity survey was made with a standard pitot-static tube rake located at various longitudinal positions along the longitudinal center line of the cavity. The pitot pressures were recorded by the wind-tunnel data acquisition system.

The acoustic data were reduced (from magnetic tape) to obtain both one-third-octave band and narrow band frequency spectra. The logarithm of the acoustic pressure (dB) is plotted against either the logarithm of frequency (one-third octave) or the linear frequency scale (narrow band). The background noise, which consisted of the acoustic noise from the flow over the closed cavity and the electronic noise from the measuring system, was subtracted from the cavity noise data at each velocity and one-third-octave

frequency. Thus, the data are displayed on a logarithmic plot as a ratio of the cavity noise to the background noise. These one-third-octave data were used for a survey of general trends.

The narrow band spectra were plotted over the frequency range from 0 to 500 Hz, with a constant band with of 1.5 Hz. The narrow-band data presented represent from 15 to 30 sec of averaged real time spectra (16 to 32 averages). The background noise was not subtracted from the narrow-band spectra, but rather is displayed together with the data.

DISCUSSION OF RESULTS

The largest pressure fluctuations of a cavity are encountered inside the cavity. Therefore, microphone 4, which was inside the cavity, could provide the best indication of whether there are oscillating pressures inside the cavity. A comparison of the far-field pressures with the pressures inside the cavity may provide a rough indication of the radiation efficiency. Recall that the one-third-octave data presented here reflect a difference between the noise level with the cavity open and the cavity closed. Since microphone 4 was flush mounted inside the cavity, the cavity-closed configuration provided meaningless reference background noise data; however, the sound pressure level differences between the cavity response for different configurations and the same microphone are realistic.

Microphones 1 and 2 were in the flow stream and were therefore subjected to a relatively high background noise level. (Microphone self-noise, generated when flow impinges on the nose cone, is considered a background noise.) These two microphones were in the acoustic near field because their distance from the cavity was on the order of a wavelength of the sound generated by the cavity. Therefore, there is no further discussion or presentation of data from these two microphones. Microphones 3 and 5 were both in the acoustic far field and these data are discussed extensively.

While data were obtained at numerous speeds from 0 to 68.6 m/sec (225 ft/sec) at intervals of 7.6 m/sec (25 ft/sec), in general, the trends can be seen with much less data. Therefore, data are presented primarily for speeds from 30.5 to 61.0 m/sec (100 to 200 ft/sec). The discussion is presented in four sections: (1) effect of velocity and comparison with theory, (2) radiation efficiency, (3) effect of upstream disturbance, and (4) effect of landing gear.

Effect of Velocity and Comparison With Theory

To obtain an overall evaluation of the cavity and far-field noise responses, one-third-octave spectra plots were made. These results from microphones 3 and 5 showed insignificant differences between configurations C, D, E, and F for speeds from 30.5 to 61.0 m/sec (100 to 200 ft/sec). This could have resulted from either a lack of source oscillations or a low signal-to-noise ratio. As a matter of interest, a comparison of narrow-band analyses of these configurations was made for speeds of 30.5 and 61.0 m/sec

(100 and 200 ft/sec). The results also indicated that the cavity noise could not be sensed by microphones 3 and 5.

Figure 4 presents the one-third-octave results for microphones 3, 4, and 5 for air speeds of 30.5 and 61.0 m/sec (100 and 200 ft/sec) and configurations D, H, I, M, and N. These configurations have the same cavity size, but have different opening and boundary-layer characteristics. These microphones in figures 4(a) and 4(b) indicate that configuration I appears to produce some tones at about 0.125 kHz. Figure 5 presents data comparisons similar to those in figure 4 except that a different basic cavity size is represented. Microphones 3, 4, and 5 seem to show some tones for configuration J at about 0.125 kHz. Configurations I (in fig. 4) and J (in fig. 5) have a partial cover over the downstream portion of the cavity. (See fig. 2.) Figure 6 shows the one-third-octave band level spectra for configuration I for tunnel speeds of 30.5, 38.1, 45.7, 53.3, and 61.0 m/sec (100, 125, 150, 175, and 200 ft/sec, respectively). The frequencies of the possible tones around 0.125 kHz illustrated in figure 6 appear to vary with speed. In particular, at 61.0 m/sec (200 ft/sec) the tones appear to center around 0.160 kHz rather than the 0.125-kHz value for the lower speeds. Thus, the differences in amplitude of the one-third-octave level appear to vary with speed. To make a more detailed evaluation of these effects, a 1.5-Hz constant bandwidth analysis of these data was performed, and the results are presented in figure 7.

Figure 7 presents frequency spectra from 0 to 500 Hz for microphones 3, 4, and 5 and for various velocities. Figures 7(a), 7(b), and 7(c) show the sound pressure level frequency spectrum for microphones 3, 5, and 4, respectively. The dashed curve in figures 7(a) and 7(b) represents the background noise. No background noise is shown in figure 7(c) because microphone 4 was in the cavity, and the background noise was measured with the cavity closed (microphone covered). The information of primary interest is the frequency at which the cavity noise is above the background data. Figure 7(c), for microphone 4, shows the fundamental cavity frequencies along with some higher harmonics.

Shown in table I(a) are the measured cavity frequencies as determined for the three microphones (3, 4, and 5) from figure 7. In table I(a), for one speed, the measured peak frequencies for the three microphones have nearly the same value, being within a few hertz of each other.

For comparison with the measured data, the lengthwise oscillation frequencies for the configuration-I cavity were calculated using three prediction methods. These methods are: (1) shear-layer oscillation associated with Nyborg's theory as modified by Spee (ref. 11); (2) feedback model associated with the Rossiter method (ref. 10); and (3) an extension of the Rossiter method that incorporated a length-to-depth ratio associatd with Block (ref. 15). A general description of these resonant conditions can be found in references 14 and 15. These natural acoustic frequencies are shown in tables I(b), I(c), and I(d), where the cavity partial covering has been disregarded. In a comparison of the results for the Nyborg mechanism as extended by Spee (shown in table I(b) and refs. 3 and 11) only one frequency seems to indicate some resemblance of prediction to measurement when using the full cavity opening in the calculations, that is, 115 Hz for a speed of 30.5 m/sec (100 ft/sec) and $m = 4$. A reduced cavity opening length was attempted (to account for the partial covering), but

the correlation between table I(a) and table I(b) was not improved. Table I(c) deals with the results of the Rossiter mechanism (ref. 10). A correlation of the computed frequencies with these measured frequencies indicates that for 38.1 m/sec (125 ft/sec), $m = 4$ seems to apply; for 45.7, 53.3, and 61.0 m/sec (150, 175, and 200 ft/sec), $m = 3$ seems to apply. Table I(d) deals with the Block prediction method presented in reference 15. Comparing the computed and measured frequencies indicates that for 30.5 and 38.1 m/sec (100 and 125 ft/sec), $n = 4$ applies well; and for 45.7, 53.3, and 61.0 m/sec (150, 175, and 200 ft/sec), $n = 3$ seems to apply reasonably well. Therefore, it can be concluded that a physical explanation is available for the measured cavity frequencies. More important, the physical explanation for these predictions is applicable to the large, full-size cavities tested in this investigation.

The partially covered cavity seems to resonate according to the Rossiter and/or Block explanation with nearly the same frequencies as the completely open cavity with the same physical dimensions. Since the partial cavity covering upstream radiates less noise than the covering downstream (see fig. 4, configurations H and I), it is concluded that the downstream covering acts as an amplifier without changing the frequency of the uncovered cavity.

Radiation Efficiency

Although there may be oscillating pressure within the cavity, this pressure may not radiate into the far field. Figure 8 presents narrow band spectra for speeds from 30.5 to 61.0 m/sec (100 to 200 ft/sec) for configuration I. The spectra for the internal cavity pressures (microphone 4) are superimposed on the spectra for the far-field pressures. Figures 8(a) and 8(b) show the sound pressure level spectrum for microphones 3 and 5, respectively. The figure shows, by a comparison of the internal and external pressure amplitudes at the peak frequencies for the various speeds, that the radiation efficiency at the given frequency (see, for example, the tone appearing between 100 and 150 Hz) varies with wind speed. Radiation efficiency is expected to also vary with the mode number which is variable in the data presented in table I. Some phase cancellation can be expected in the far field for the higher harmonics.

Effect of Upstream Disturbance

The boundary layer over the cavity is known to affect the noise radiation on a model scale (see refs. 14 and 16). To evaluate this effect for full scale, turbulence generators were placed on the upstream edge of the cavity. In addition, a velocity survey was performed to evaluate the actual boundary layer over the cavity (i.e., to measure the effectiveness of the false floor). These surveys were made without any upstream disturbances fastened to the cavity.

The results of the velocity survey are shown in figures 9 and 10. The coordinate system used to describe the velocity survey coordinates is shown in figure 3. The general rake location is shown on the insert in figures 9 and 10. *Figure 9(a) (velocity survey at the leading edge of the false floor and for the* cavity completely open) shows that the boundary-layer thickness is less than about 1 cm (0.4 in.) and that the false floor was effective in keeping the

wind-tunnel floor boundary layer from affecting the flow over the cavity. A comparison of figures 9(a), 9(b), and 9(c) shows the buildup in the boundary layer as the air moves down along the flase floor toward and over the cavity. A comparison of figures 9(d) and 10 shows the velocity distribution for the probe at the same position over the cavity with the cavity open and closed. At the higher speeds there is a significant difference between the velocity profiles. A comparison of figures 9(c) and 9(d) indicates that most of the momentum lost at the upstream end of the cavity is recovered further downstream.

To evaluate the upstream disturbance effects on the cavity noise, configurations K, L, M, and N were tested. The one-third-octave spectra differences for cavities of the same size, both without a turbulence generator, configuration I, and with two different turbulence generators, configurations M and N, are shown in figure 4. The data show that changing the boundary layer with turbulence generators tends to decrease the amplitude of the tones (frequency at about 0.125 Hz) for both forward speeds (figs. 4(a) and 4(b)).

For a cavity of different size (configuration J without turbulence generators), figure 5 shows that changing the boundary layer with turbulence generators again decreases the amplitude of the tones (frequencies at 0.1000 and 0.125 kHz) for both forward speeds. Therefore, it is concluded from figures 4 and 5 that introducing upstream disturbance, which among other things increases the boundary-layer thickness, tends to decrease the amplitude of the cavity noise level.

Effect of Landing Gear

To evaluate the effect of a landing-gear strut on the cavity noise, a tall, narrow board was fastened at the center line of the downstream or upstream vertical walls of the cavity. (See fig. 2 for configurations P and Q, respectively.) Figure 11 presents one-third-octave band sound pressure level spectra for a cavity with (configurations P and Q) and without (configuration D) the strut for tunnel speeds of 30.5 and 61.0 m/sec (100 and 200 ft/sec). The data in figures 11(a) and 11(b) for microphone 4 show only moderate differences between the levels for the configuration without the strut (configuration D) and with the strut on the downstream cavity wall (configuration P). However, with the strut in the forward position (configuration Q) an appreciable difference is noticeable. The data in figures 11(a) and 11(b) for microphones 3 and 5, however, did not show the difference revealed in the data for microphone 4. Recall that microphones 3 and 5 were in the far field whereas microphone 4 was flush with the inside side wall (in a forward section of the cavity). Therefore, microphone 4 was physically close to the position of the strut inside of the cavity (see the microphone coordinates in fig. 3). Two possible explanations are offered for the differences between microphones 3 and 5 and microphone 4 in figure 11. First, the background noise level is above that of the strut and cavity level. This difference is deduced from the near zero difference in decibel level shown for microphones 3 and 5. The second explanation is that for configuration Q, microphone 4 is very close to the simulated strut, and therefore is subjected to aerodynamic pressure fluctuations or structural resonances that may not have radiated noise. The small

differences between the microphone 4 levels for configurations D and P compared with the large differences between configurations D and Q seem to favor the second argument.

CONCLUDING REMARKS

Acoustic measurements of a large scale cavity have been made with inside and far-field microphones. The measured frequencies have been compared with frequencies derived from available theories previously correlated with small scale models. There is some correlation for the large cavity tested which indicates that existing theories are applicable over a broader range than previously shown. A qualitative evaluation of the cavity radiation efficiency indicates that acoustic radiation varies with speed and mode number. The cavity configuration with the partial covering downstream seems to amplify the tonal intensities. The frequency of the tones seems to depend on cavity size and not cavity open area. Introducing upstream disturbance seems to decrease the amplitude of the cavity tones.

Langley Research Center
National Aeronautics and Space Administration
Hampton, VA 23665
April 5, 1978

REFERENCES

1. Hardin, Jay C.; Fratello, David J.; Hayden, Richard E.; Kadman, Yoran; and Africk, Steven: Prediction of Airframe Noise. NASA TN D-7821, 1975.

2. Gibson, John S.: The Ultimate Noise Barrier - Far Field Radiated Aerodynamic Noise. Inter-Noise 72 Proceedings, Malcolm J. Crocker, ed., Inst. Noise Control Eng., c.1972, pp. 332-337.

3. Nyborg, Wesley L.: Self-Maintained Oscillations of the Jet in a Jet-Edge System. I. J. Acoust. Soc. America, vol. 26, no. 2, Mar. 1954, pp. 174-182.

4. Krishnamurty, K.: Acoustic Radiation From Two-Dimensional Rectangular Cutouts in Aerodynamic Surfaces. NACA TN 3487, 1955.

5. Roshko, Anatol: Some Measurements of Flow in a Rectangular Cutout. NACA TN 3488, 1955.

6. Dunham, William H.: Flow-Induced Cavity Resonance in Viscous Compressible and Incompressible Fluids. Fourth Symposium on Naval Hydrodynamics - Propulsion Hydroelasticity, ACR-92, Aug. 1962, pp. 1057-1081.

7. Harrington, M. C.; and Dunham, W. H.: Studies of the Mechanism for the Flow-Induced Cavity Resonance. J. Acoust. Soc. America, vol. 32, no. 7, July 1960, p. 921.

8. Plumblee, H. E.; Gibson, J. S.; and Lassiter, L. W.: A Theoretical and Experimental Investigation of the Acoustic Response of Cavities in an Aerodynamic Flow. WADD-TR-61-75, U.S. Air Force, Mar. 1962.

9. Maull, D. J.; and East, L. F.: Three-Dimensional Flow in Cavities. J. Fluid Mech., vol. 16, pt. 4, Aug. 1963, pp. 620-632.

10. Rossiter, J. E.: Wind-Tunnel Experiment on the Flow Over Rectangular Cavities at Subsonic and Transonic Speeds. R. & M. No. 3438, British A.R.C., Oct. 1964.

11. Spee, B. M.: Wind Tunnel Experiments on Unsteady Cavity Flow at High Subsonic Speeds. Separated Flows, Part II, AGARD CP No. 4, May 1966, pp. 941-974.

12. Heller, H. H.; Holmes, D. G.; and Covert, E. E.: Flow-Induced Pressure Oscillations in Shallow Cavities. J. Sound & Vib., vol. 18, no. 4, Oct. 1971, pp. 545-553.

13. Heller, Hanno H.; and Bliss, Donald B.: The Physical Mechanism of Flow-Induced Pressure Fluctuations in Cavities and Concepts for Their Suppression. AIAA Paper 75-491, Mar. 1975.

14. Block, Patricia J. W.; and Heller, Hanno: Measurements of Farfield Sound Generated From a Flow-Excited Cavity. NASA TM X-3292, 1975.

15. Block, Patricia J. W.: Noise Response of Cavities of Varying Dimensions at Subsonic Speeds. NASA TN D-8351, 1976.

16. DeMetz, F. C.; and Farabee, T. M.: Laminar and Turbulent Shear Flow Induced Cavity Resonances. AIAA Paper 77-1293, Oct. 1977.

17. Block, P. J. W.: Measurements of the Tonal Component of Cavity Noise and Comparison With Theory. NASA TP-1013, 1977.

TABLE I.- MEASURED AND THEORETICAL CAVITY FREQUENCIES

(a) Configuration I

V		Measured fundamental frequencies, Hz, for -		
m/sec	ft/sec	Microphone 5 (fig. 7(b))	Microphone 3 (fig. 7(a))	Microphone 4 (fig. 7(c))
30.5	100	115	120	113
38.1	125	132	128	133
45.7	150	115	114	115
53.3	175	128	127	128
61.0	200	143	141	142

(b) Configuration I (theoretical; Spee, ref. 11)

V		Theoretical natural frequency, Hz, as predicted for -				
m/sec	ft/sec	m = 1	m = 2	m = 3	m = 4	m = 5
L = 0.589 m (1.932 ft)						
30.5	100	37.01	63.63	89.81	115.86	141.84
38.1	125	46.26	79.54	112.26	144.82	177.3
45.7	150	55.52	95.44	134.7	173.78	212.76
53.3	175	64.77	111.35	157.17	202.75	248.22
61.0	200	74.02	127.26	179.62	231.71	283.68
With a reduced L; L = 0.392 m (1.286 ft)						
30.5	100		95.57	134.90	174.02	213.05
38.1	125		119.47	168.62	217.52	266.31
45.7	150	83.39	143.35	202.32	261.02	
53.3	175	97.29	167.25	236.07	304.54	
61.0	200	116.18	191.15			

TABLE I.- Concluded

(c) Configuration I (theoretical; Rossiter, ref. 10)

$$f_m = \frac{V(m - \alpha)}{L\left(\frac{1}{K_V} + m\right)}; \quad L = 0.589 \text{ m } (1.932 \text{ ft}); \quad \alpha = 0.25; \quad K_V = 0.57$$

V		Theoretical natural frequencies, Hz, as predicted for -					
m/sec	ft/sec	m = 1	m = 2	m = 3	m = 4	m = 5	m = 6
30.5	100	21.09	49.21	77.33	105.45	133.57	161.69
38.1	125	26.05	60.79	95.53	130.27	165.00	199.74
45.7	150	30.91	72.12	113.33	154.54	195.75	236.96
53.3	175	35.65	83.18	130.72	178.25	235.78	273.3
61.0	200	40.29	94.00	147.72	201.4	255.1	208.87

(d) Configuration I (theoretical; Block, ref. 15)

$$f_n = \frac{nM}{\frac{L}{cK_V} + M\frac{L}{c}\left(1 + \frac{0.514}{L/D}\right)}; \quad c = \text{Speed of sound, m/sec (ft/sec)};$$

$D = 0.460$ m (1.510 ft); $L = 0.589$ m (1.932 ft);
M = Mach number

V		Theoretical natural frequencies, Hz, as predicted for -		
m/sec	ft/sec	n = 2	n = 3	n = 4
30.5	100	58	86	115
38.1	125	71	106	141
45.7	150	83	125	167
53.3	175	96	144	191
61.0	200	108	162	215

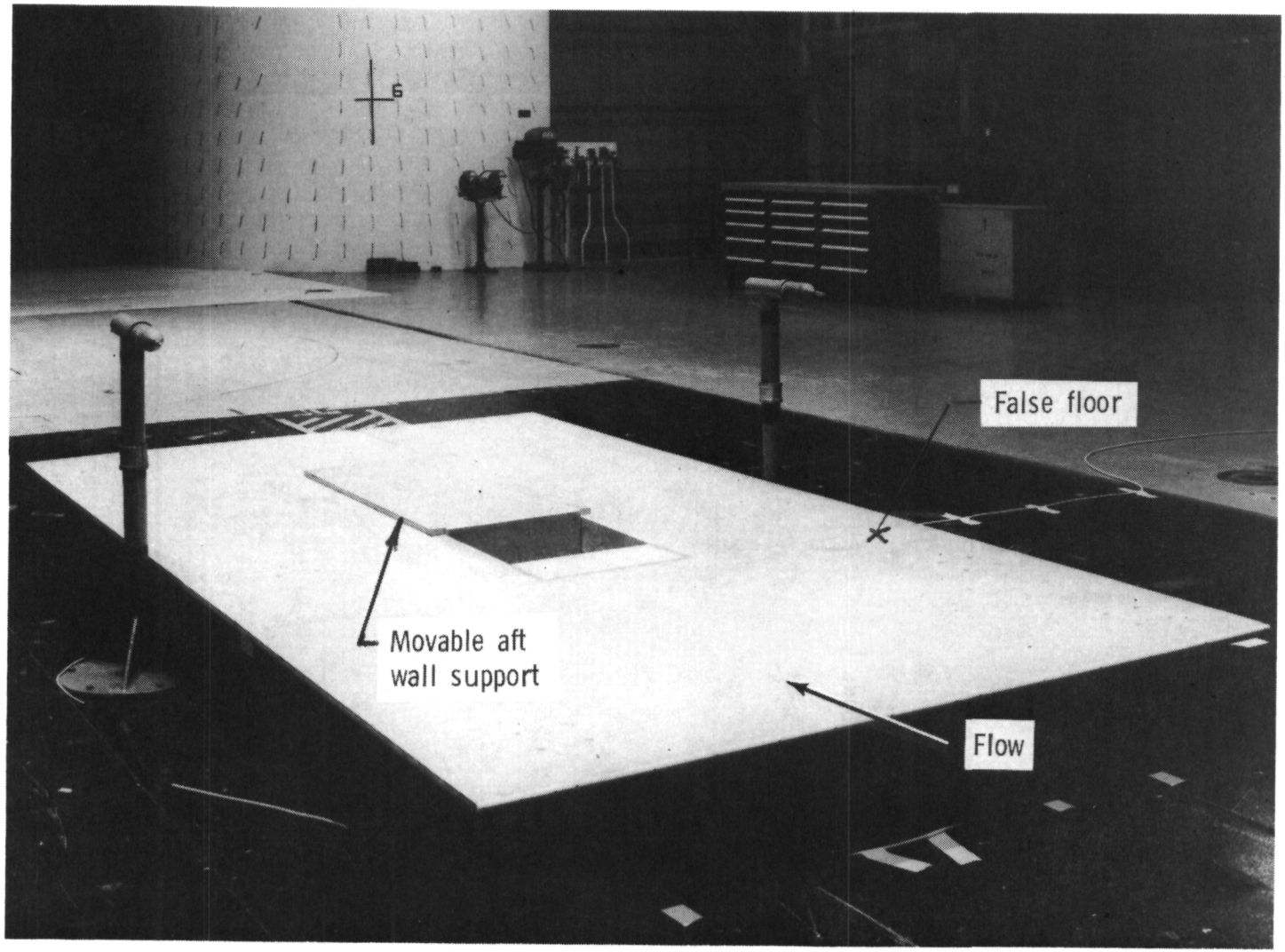

L-76-2202.1

Figure 1.- Photograph of cavity in Langley V/STOL tunnel.

Configuration	Length, cm (in.)	Depth, cm (in.)
A	0	0
B	99.8 (39.3)	46.0 (18.1)
C	39.4 (15.5)	46.0 (18.1)
D	58.9 (23.2)	46.0 (18.1)
E	78.7 (31.0)	46.0 (18.1)
F	99.8 (39.3)	23.1 (9.1)

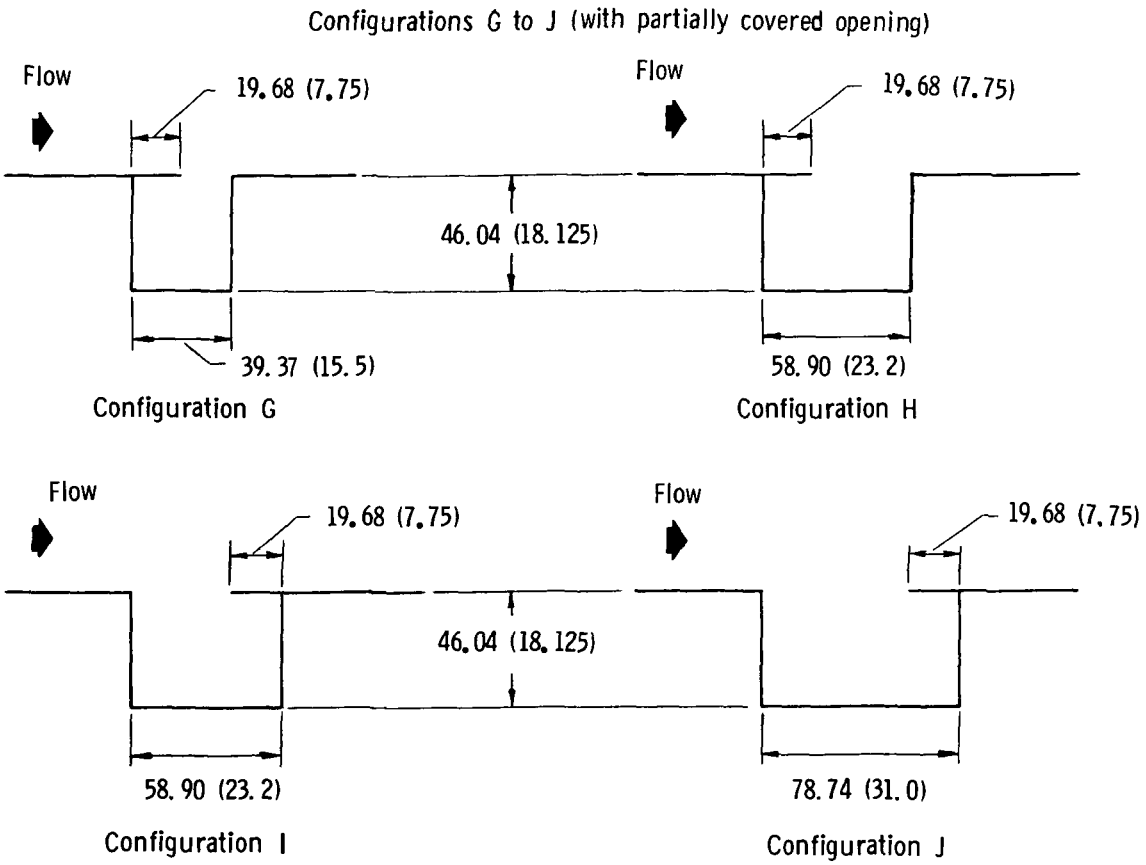

Figure 2.- Model cavity configurations. Cavity width for all models was 43.18 cm (17 in.); all dimensions are in cm (in.).

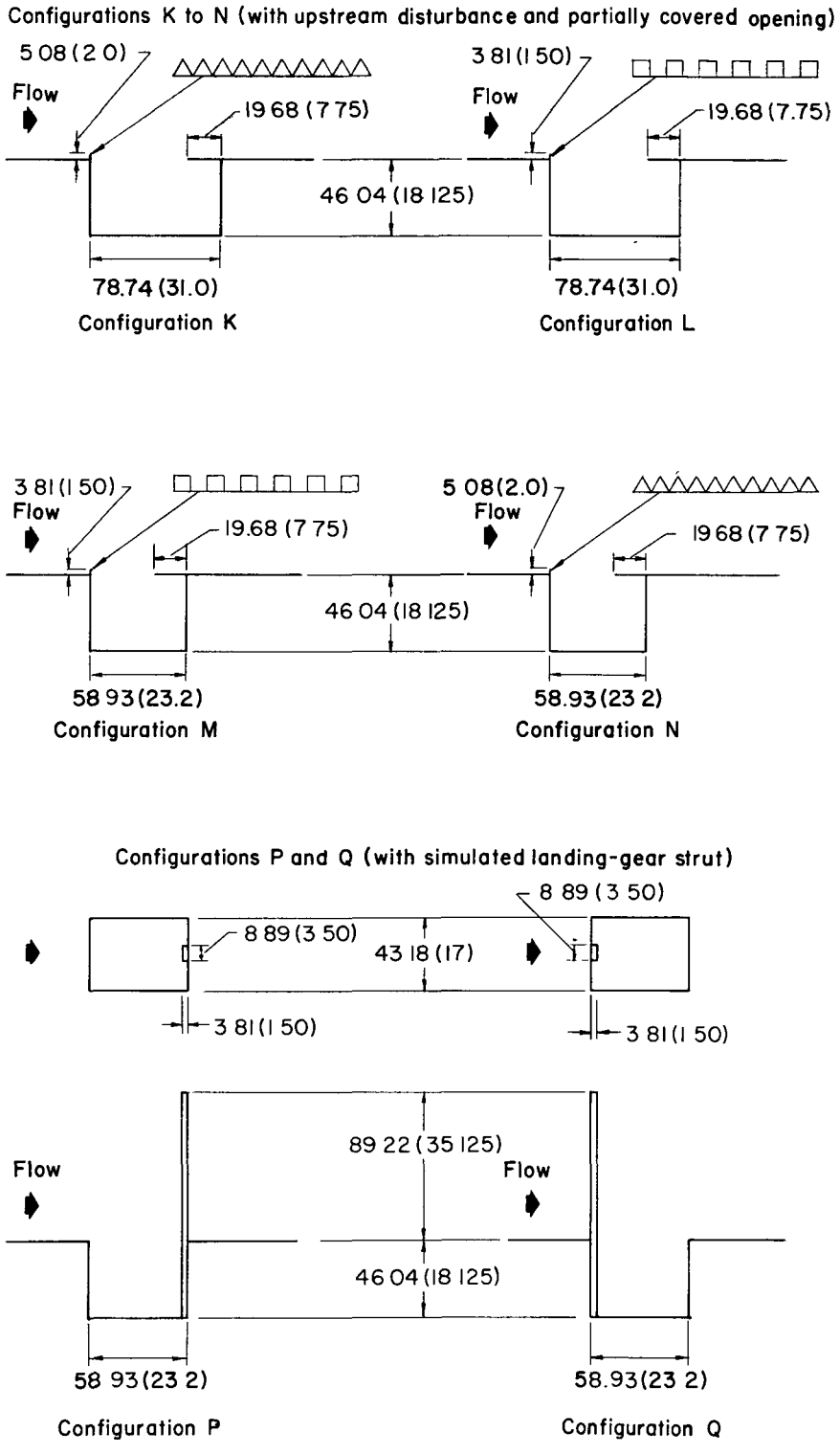

Figure 2.- Concluded.

	x	y	z
Microphone			
1	0.499 (1.638)	1.041 (3.417)	0.6096 (2)
2	.499 (1.638)	-1.033 (-3.390)	.6096 (2)
3	≈ 0	-7.010 (-23.000)	4.928 (16.167)
4	.133 (.4375)	-.216 (-.7083)	-.051 (-.167)
5	.522 (1.713)	.432 (1.417)	7.010 (23)

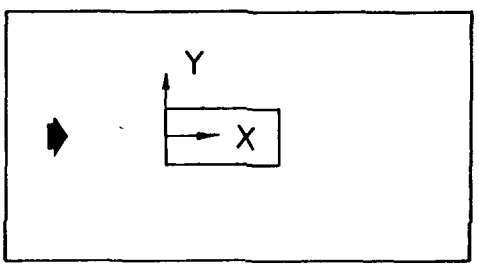

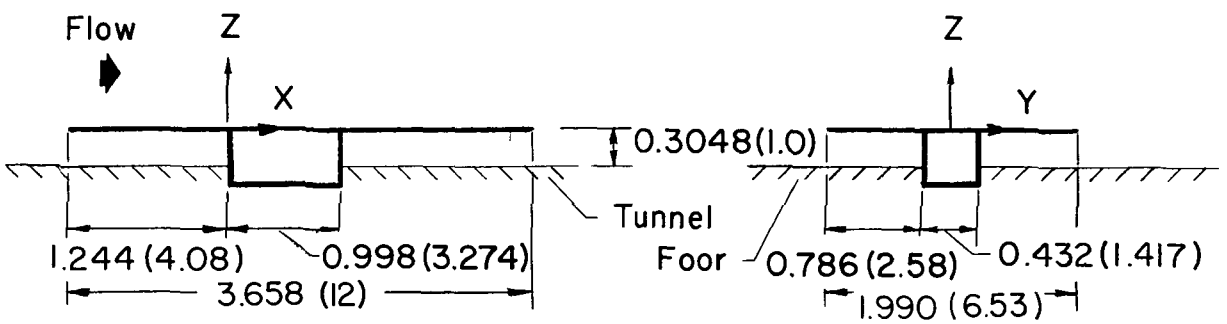

Figure 3.- Microphone coordinates, m (ft).

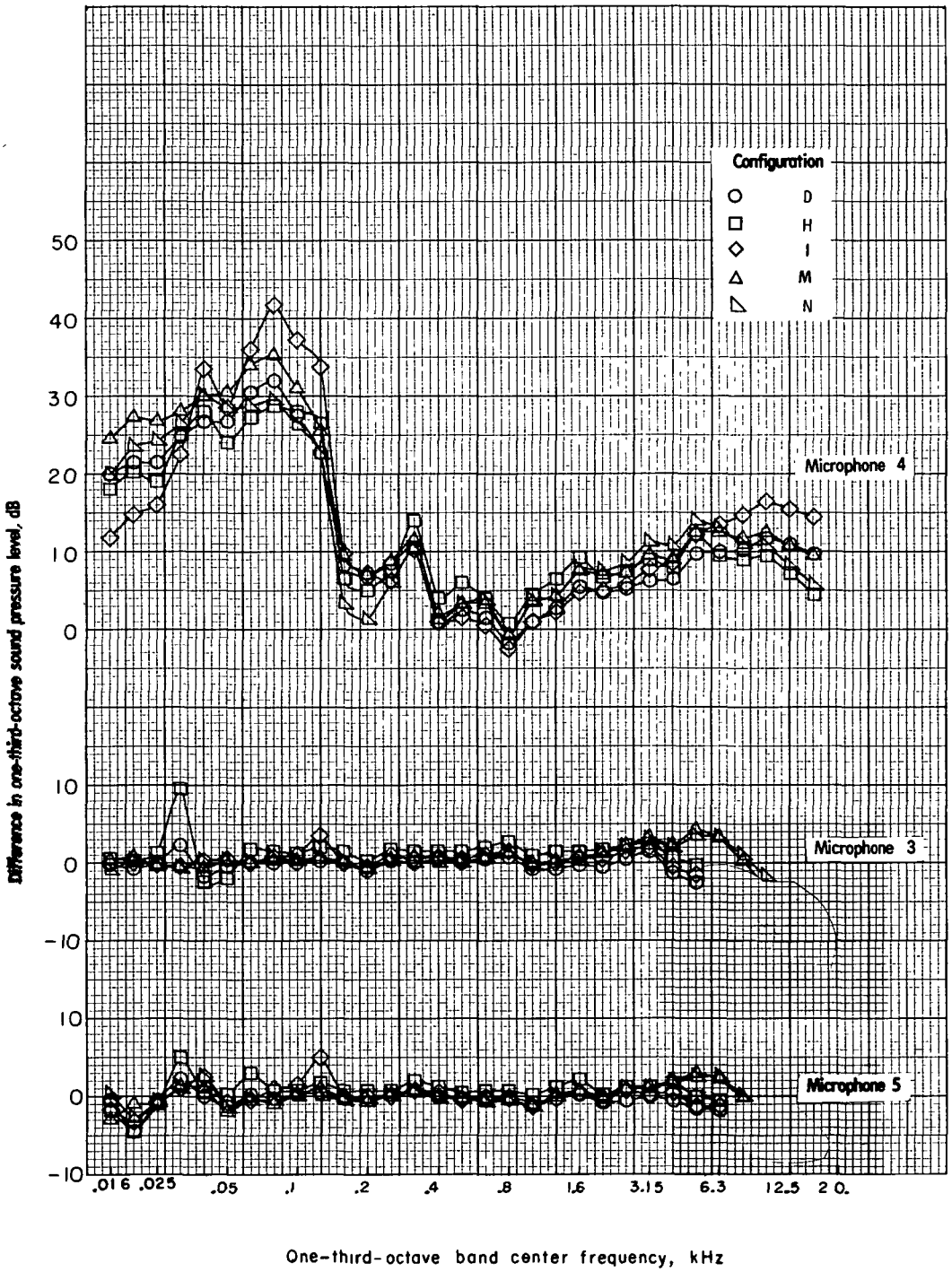

(a) 30.5 m/sec (100 ft/sec).

Figure 4.- Differences in one-third-octave sound pressure levels for one cavity size and different open area characteristics for two forward speeds.

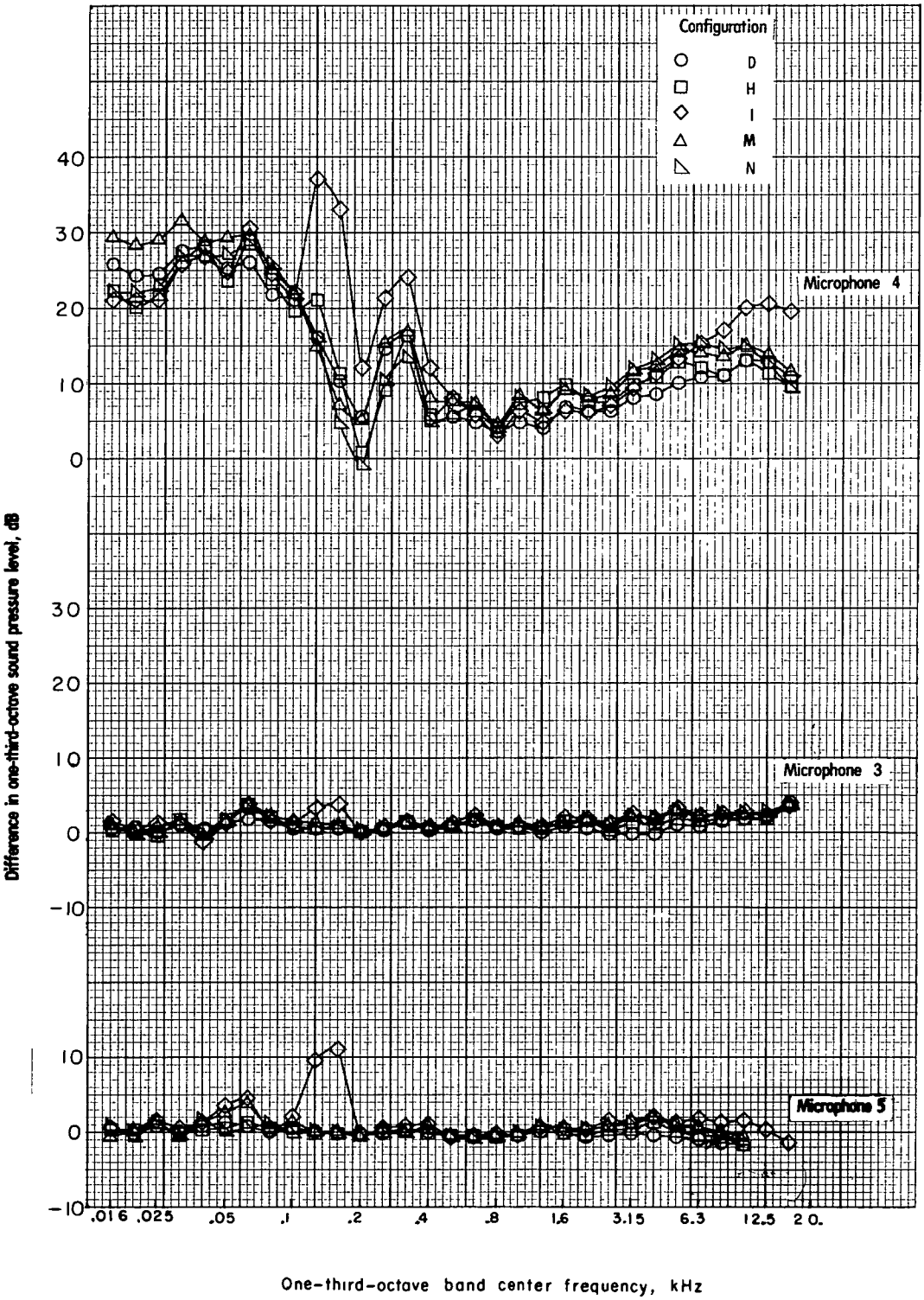

(b) 61.0 m/sec (200 ft/sec).

Figure 4.- Concluded.

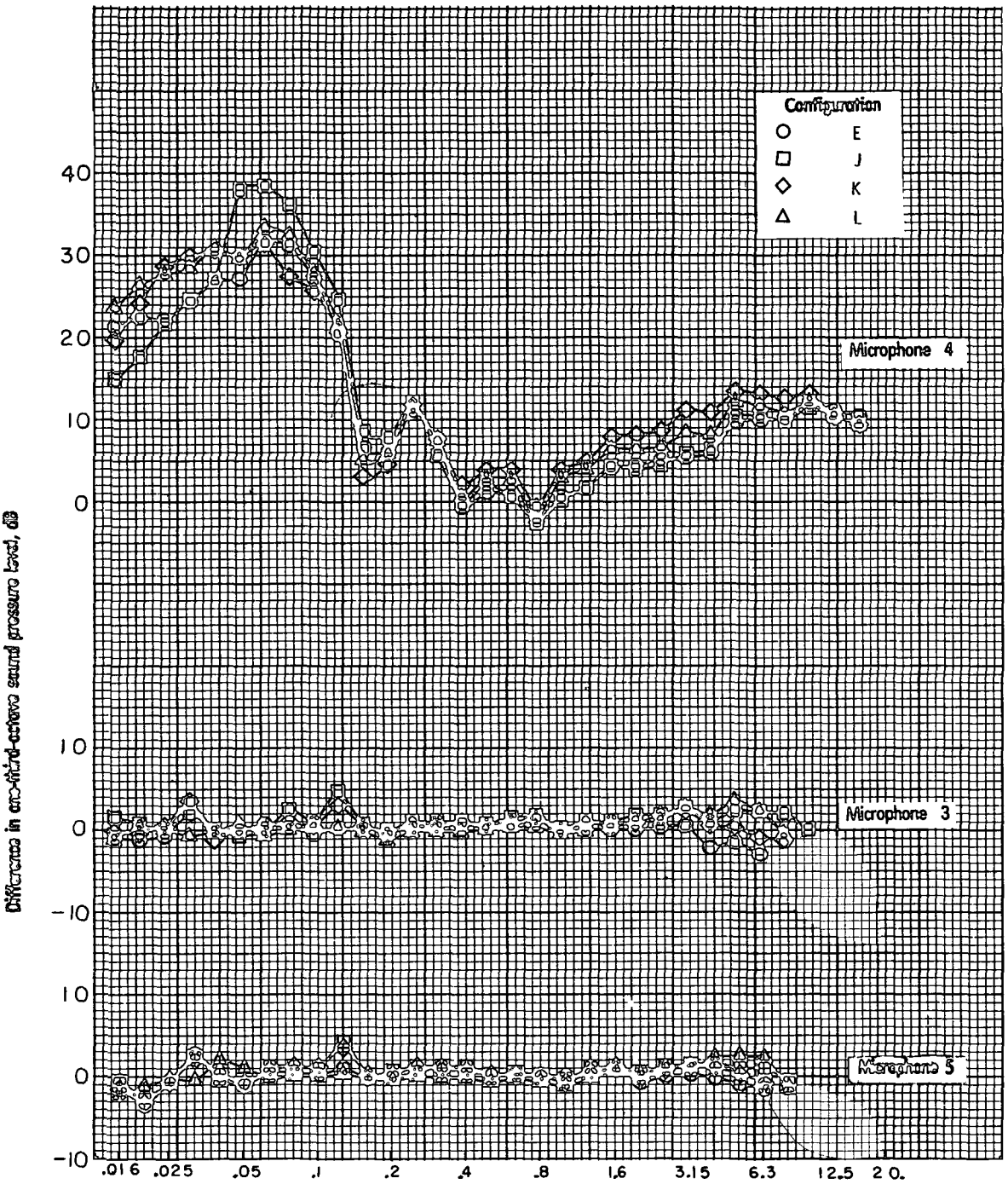

(a) 30.5 m/sec (100 ft/sec).

Figure 5.- Differences in one-third-octave sound pressure levels for one cavity size and different open area characteristics for two forward speeds.

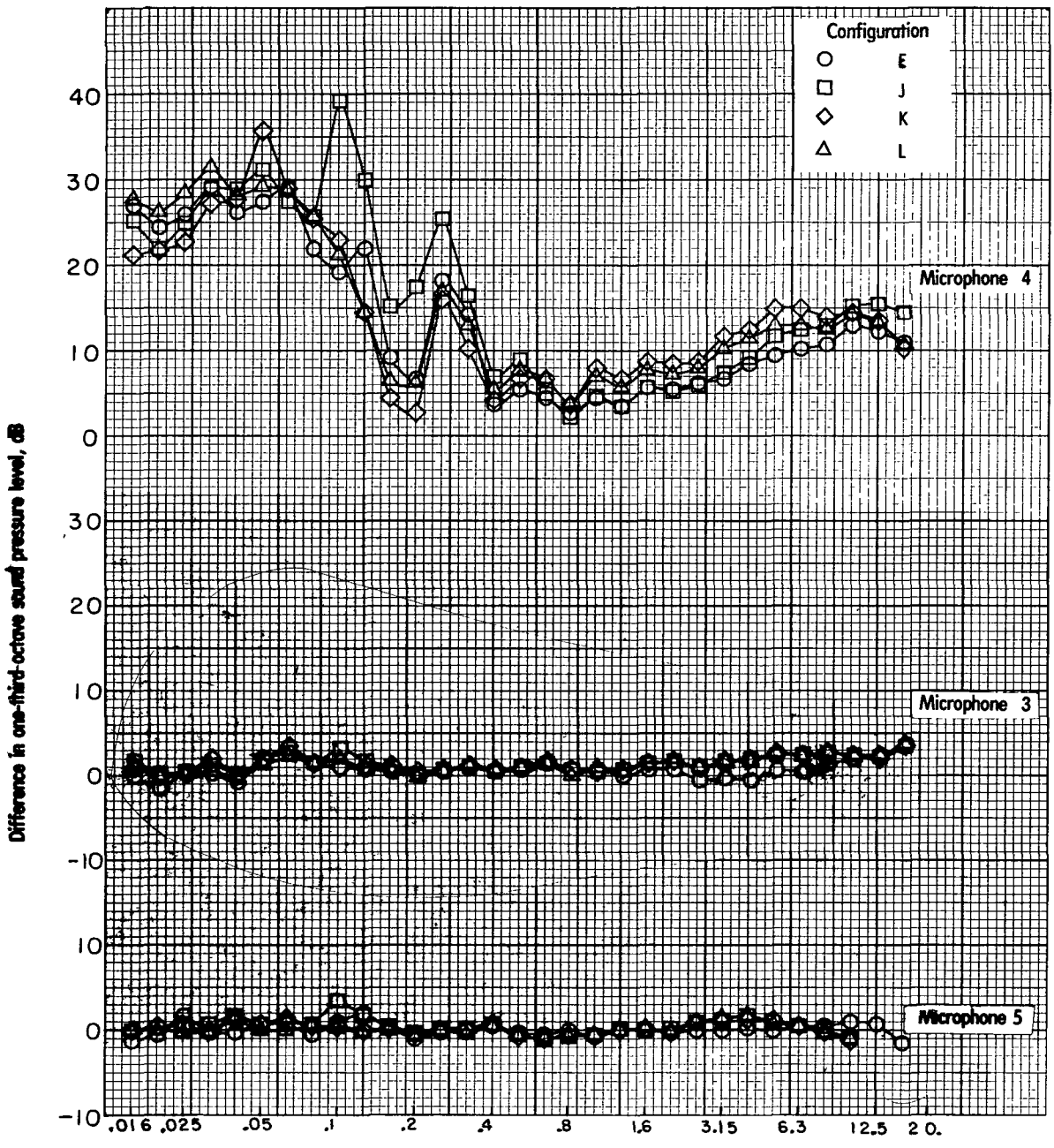

(b) 61.0 m/sec (200 ft/sec).

Figure 5.- Concluded.

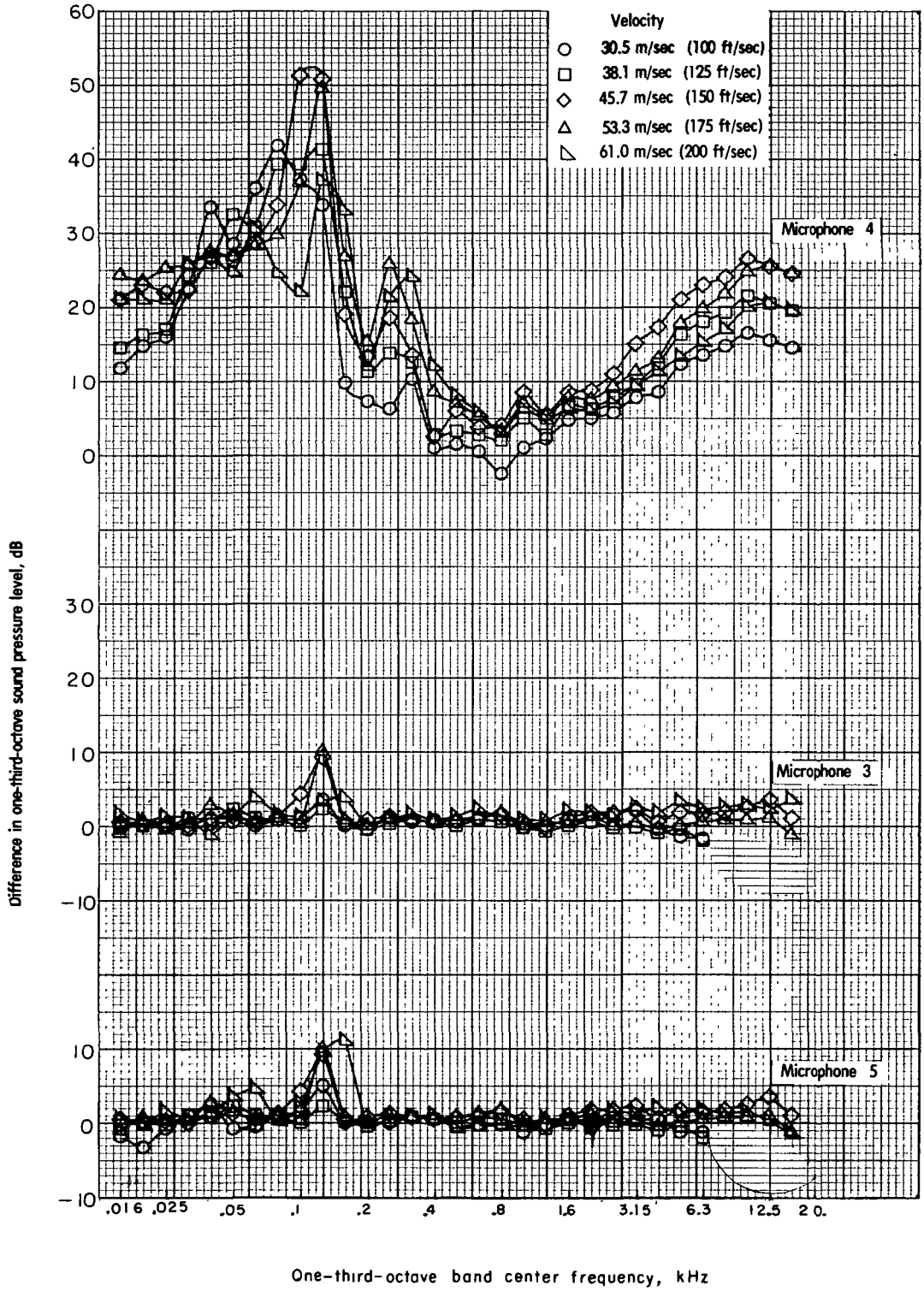

Figure 6.- Differences in one-third-octave sound pressure levels for configuration I as function of forward speed.

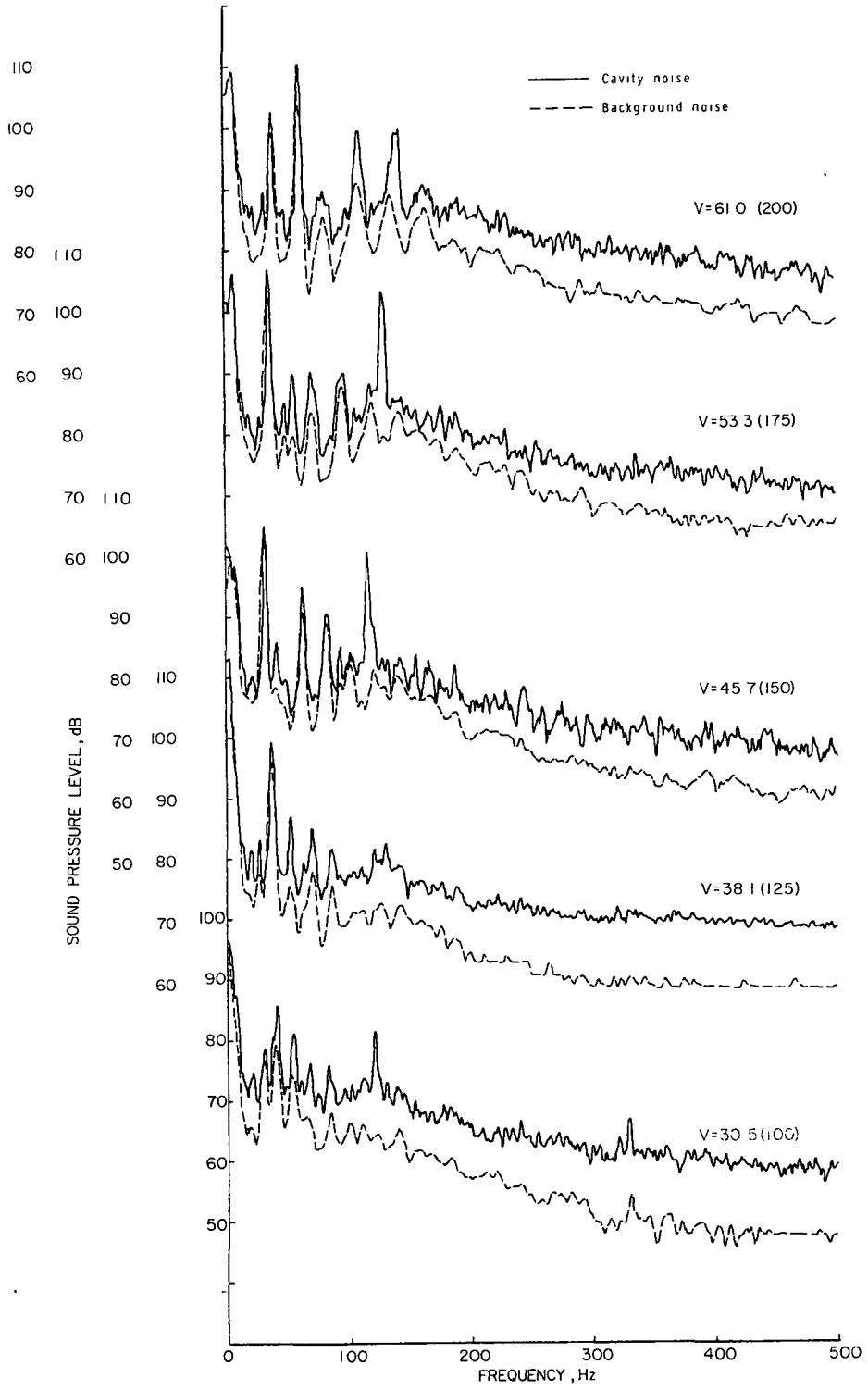

(a) Microphone 3.

Figure 7.- Sound and pressure level frequency spectrum for configuration I as function of forward speed for microphones 3, 4, and 5. V is measured in m/sec (ft/sec).

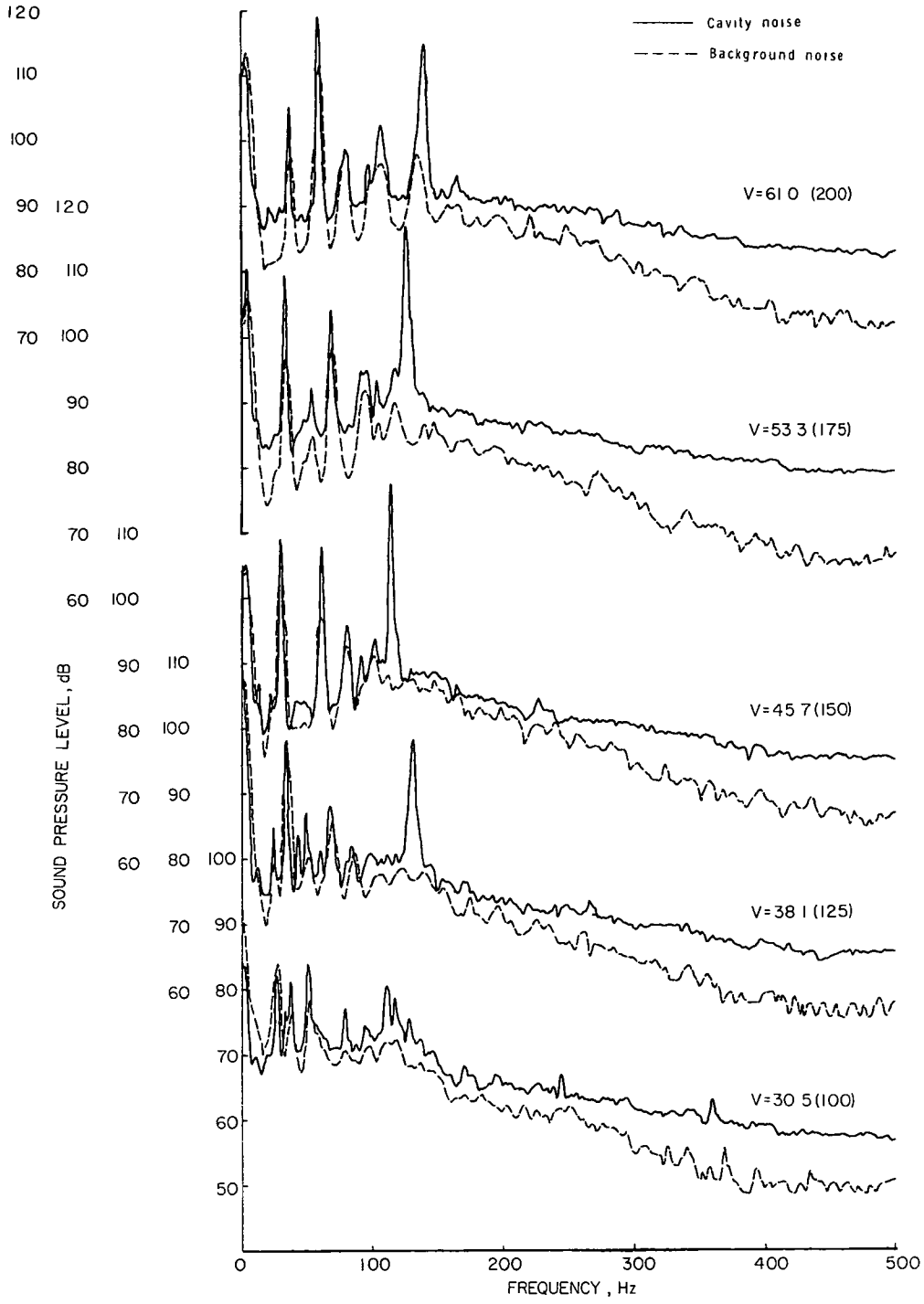

(b) Microphone 5.

Figure 7.- Continued.

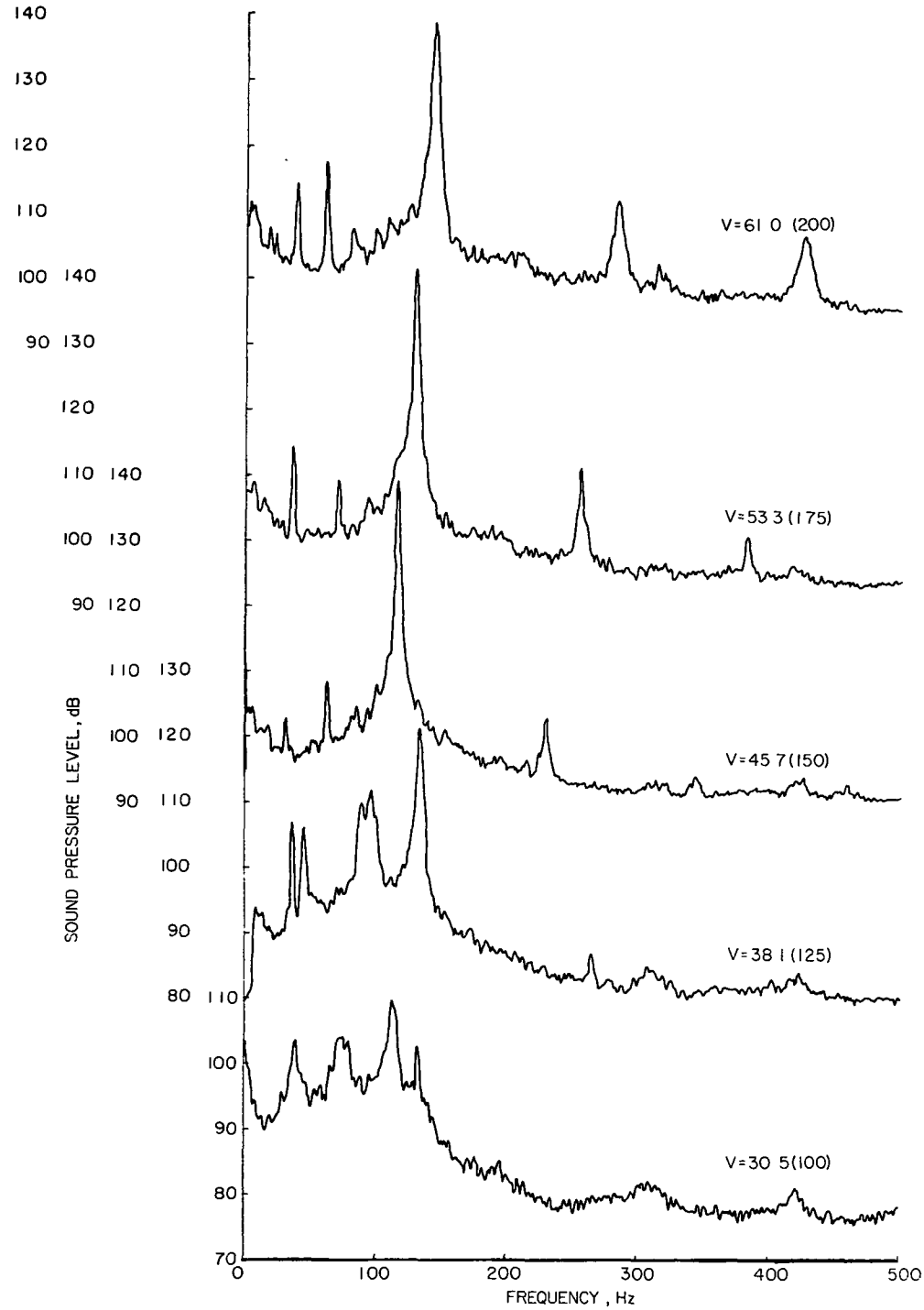

(c) Microphone 4.

Figure 7.- Concluded.

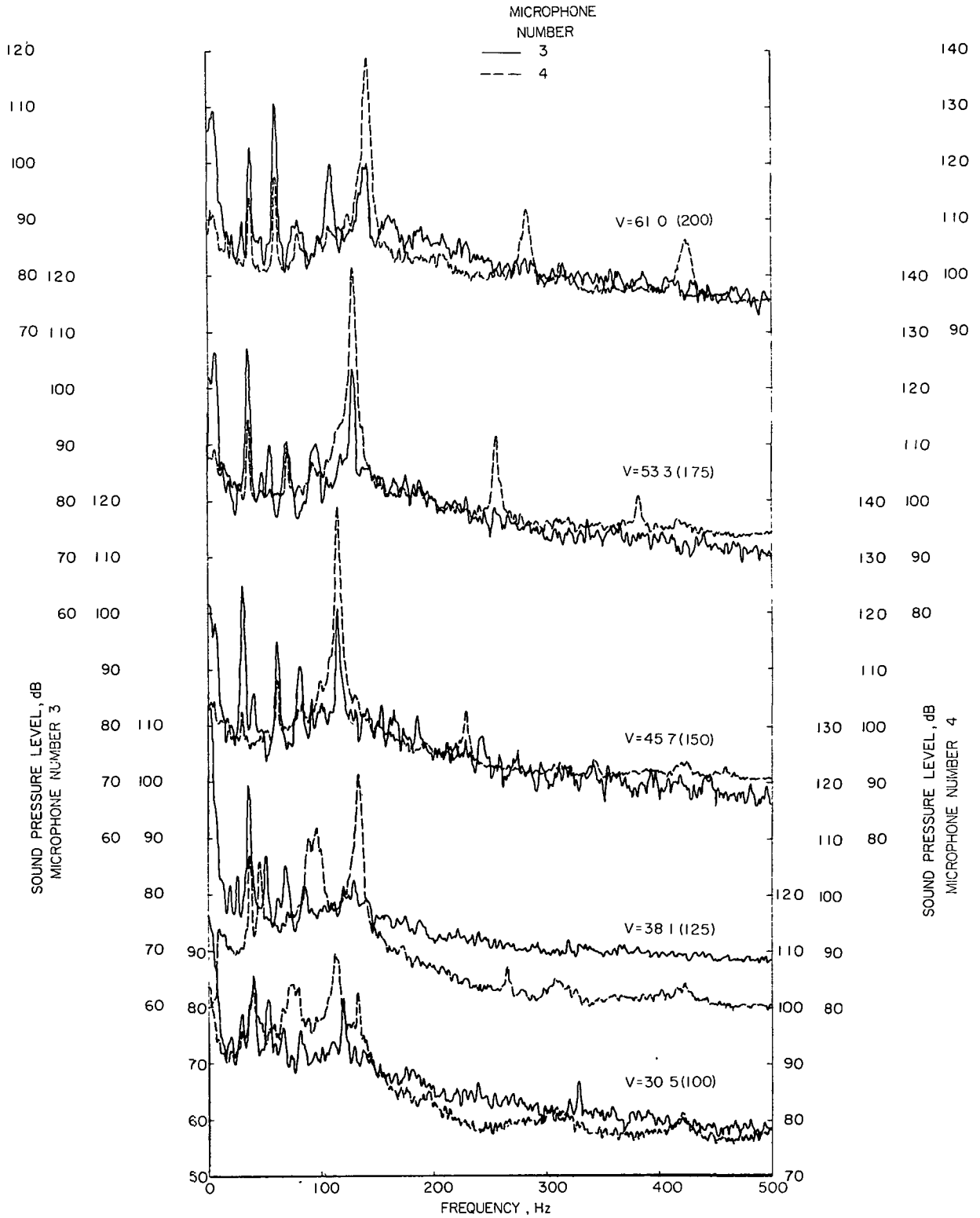

(a) Microphone 3.

Figure 8.- Narrow band sound pressure spectrum comparison of internal (microphone 4) and far-field pressures (microphones 3 and 5) for configuration I. V is measured in m/sec (ft/sec).

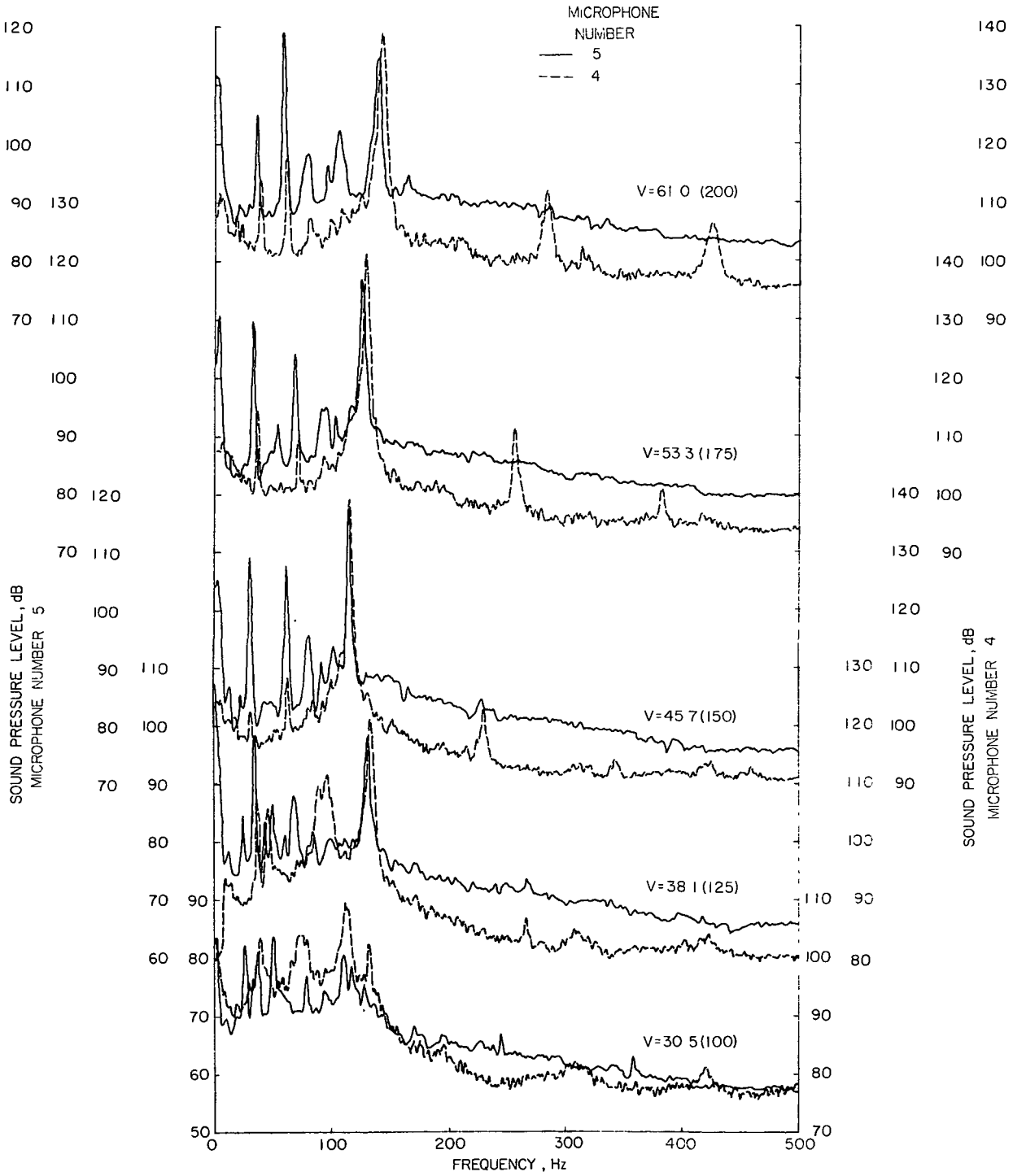

(b) Microphone 5.

Figure 8.- Concluded.

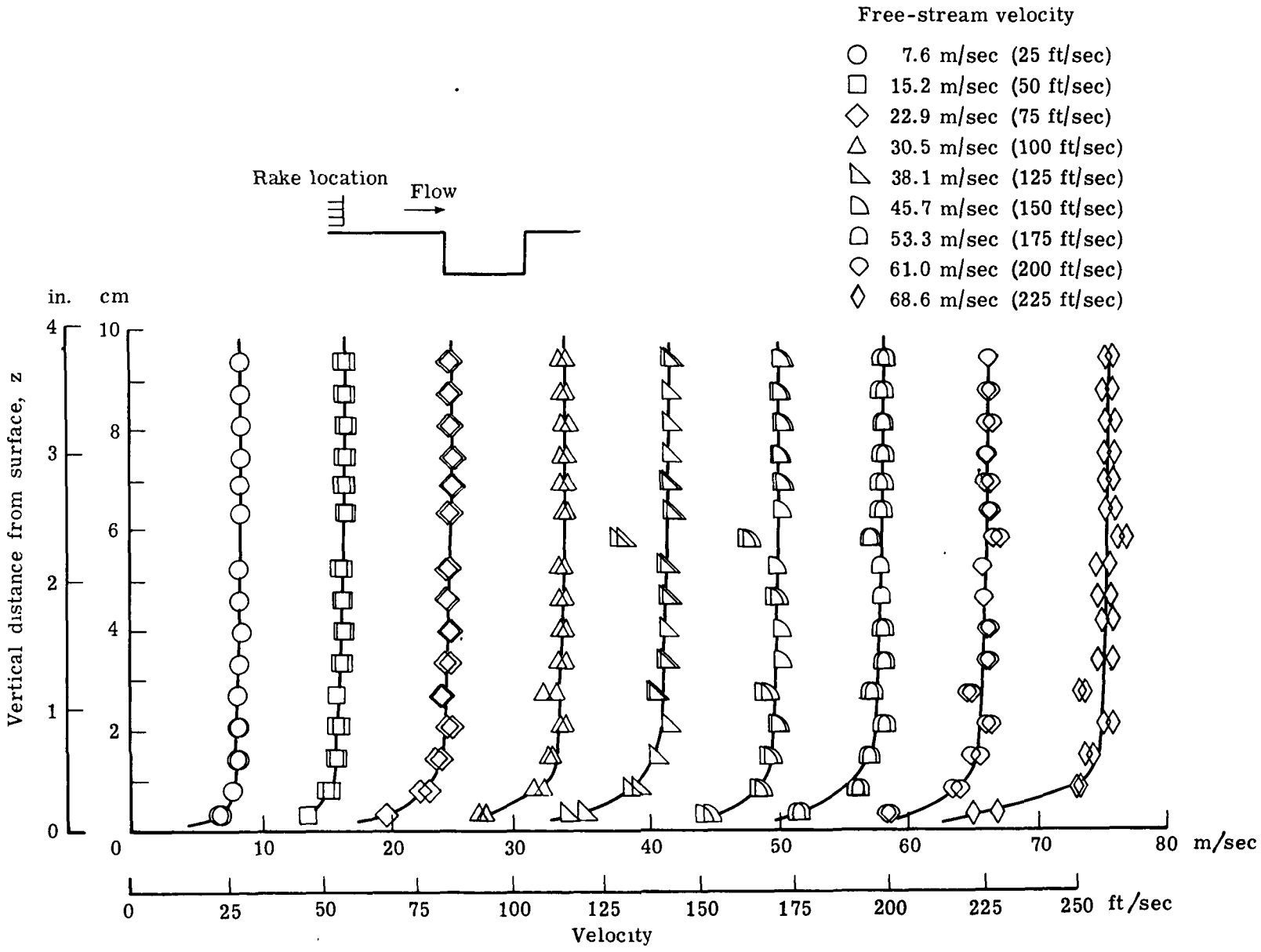

(a) Configuration B; x = -124.9 cm (-49.1 in.); y = 0.

Figure 9.- Velocity survey over open cavity.

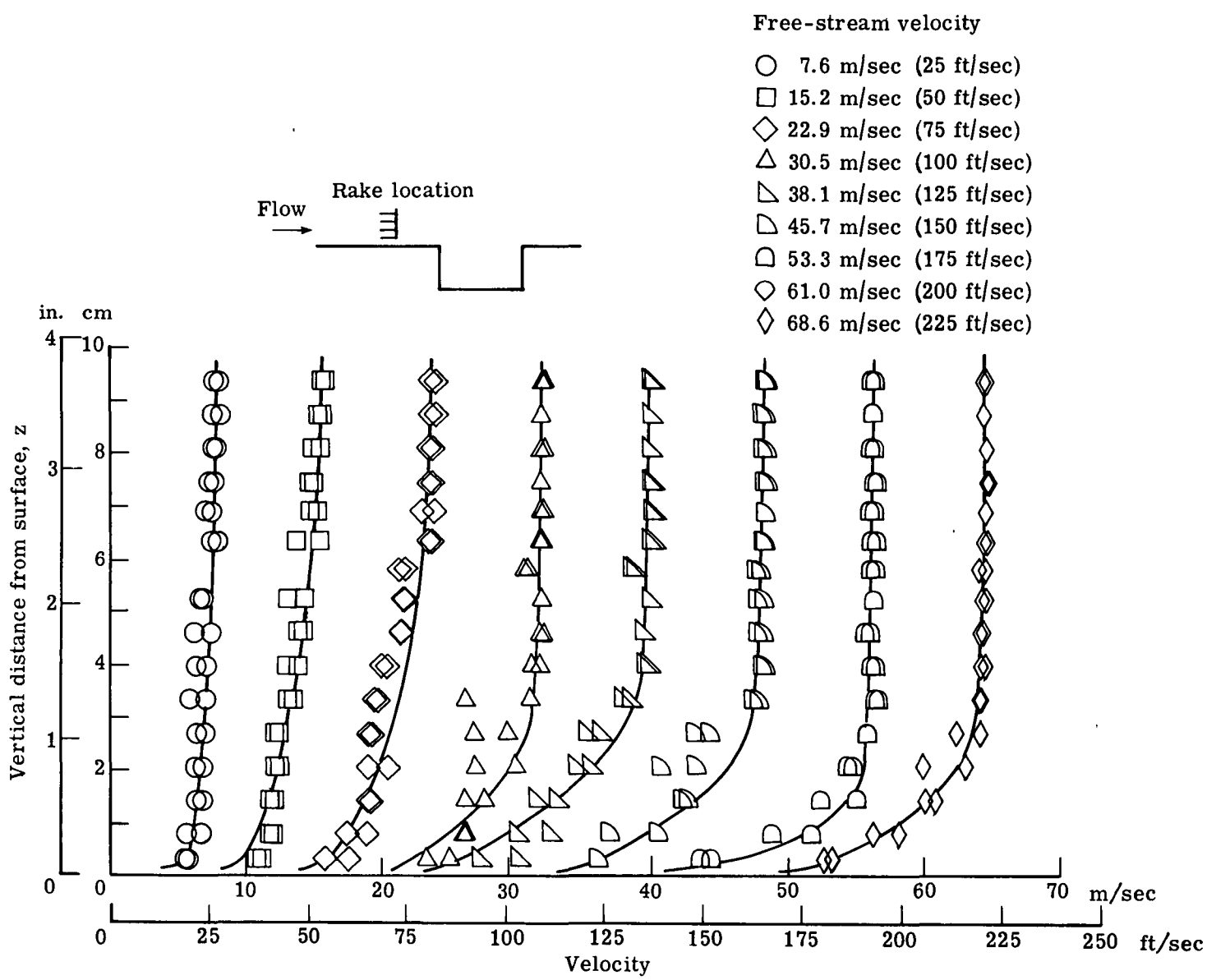

(b) Configuration B; x = -74.4 cm (-29.3 in.); y = 0.

Figure 9.- Continued.

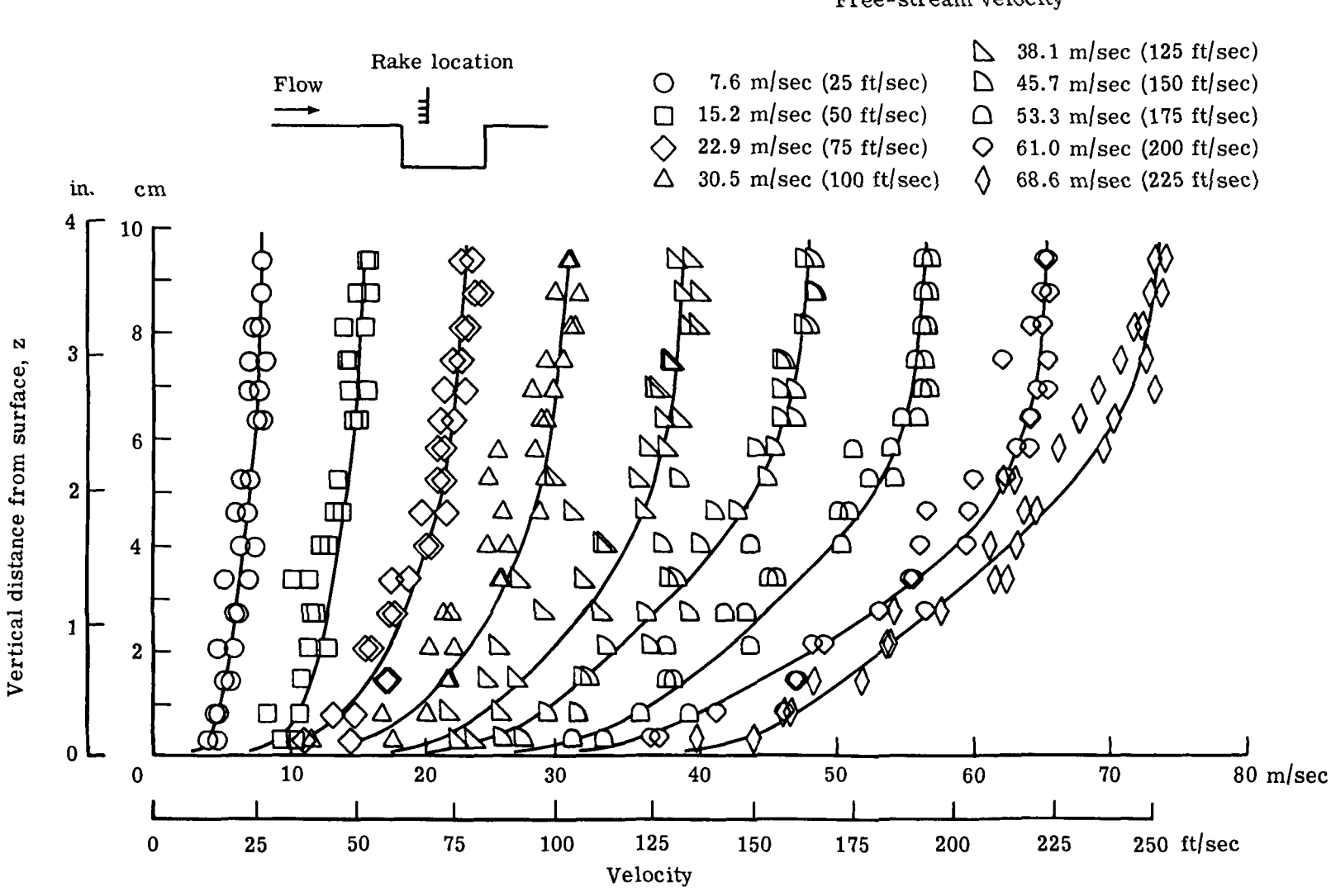

(c) Configuration B; x = 62.7 cm (24.7 in.); y = 0.

Figure 9.- Continued.

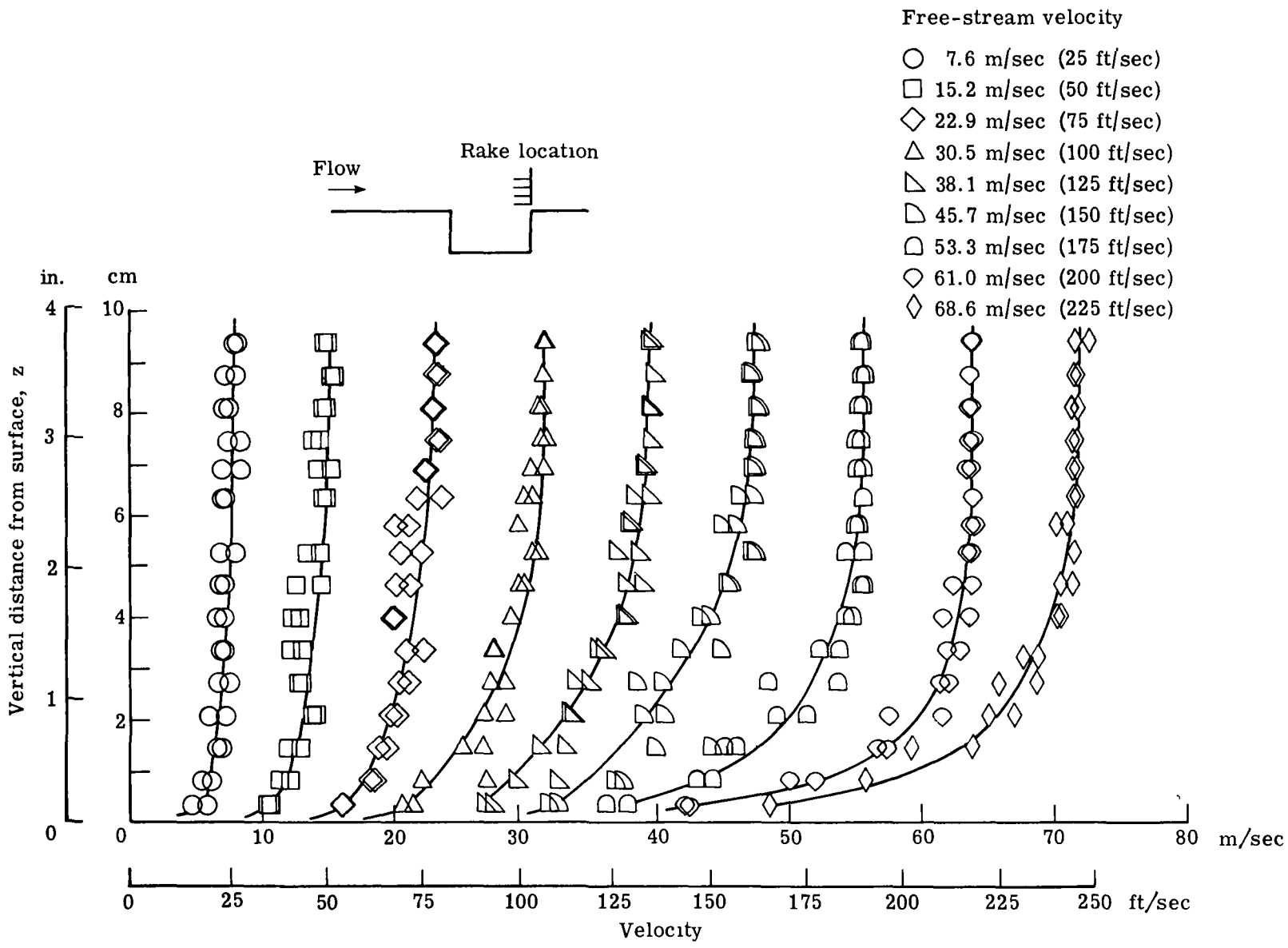

(d) Configuration B; x = 77.5 cm (30.5 in.); y = 0.

Figure 9.- Concluded.

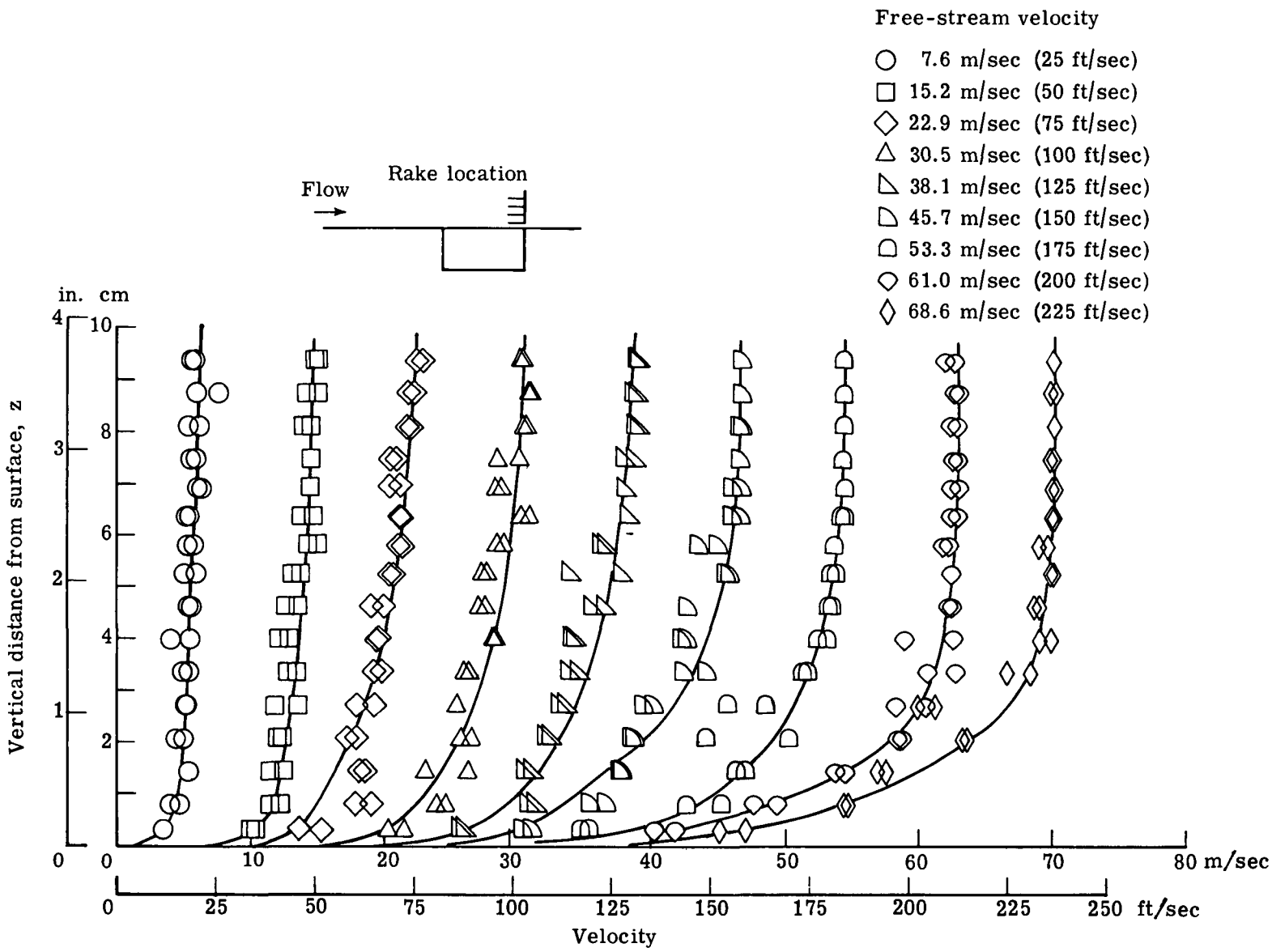

Figure 10.- Velocity survey over closed cavity; configuration A;
x = 77.5 cm (30.5 in.); y = 0.

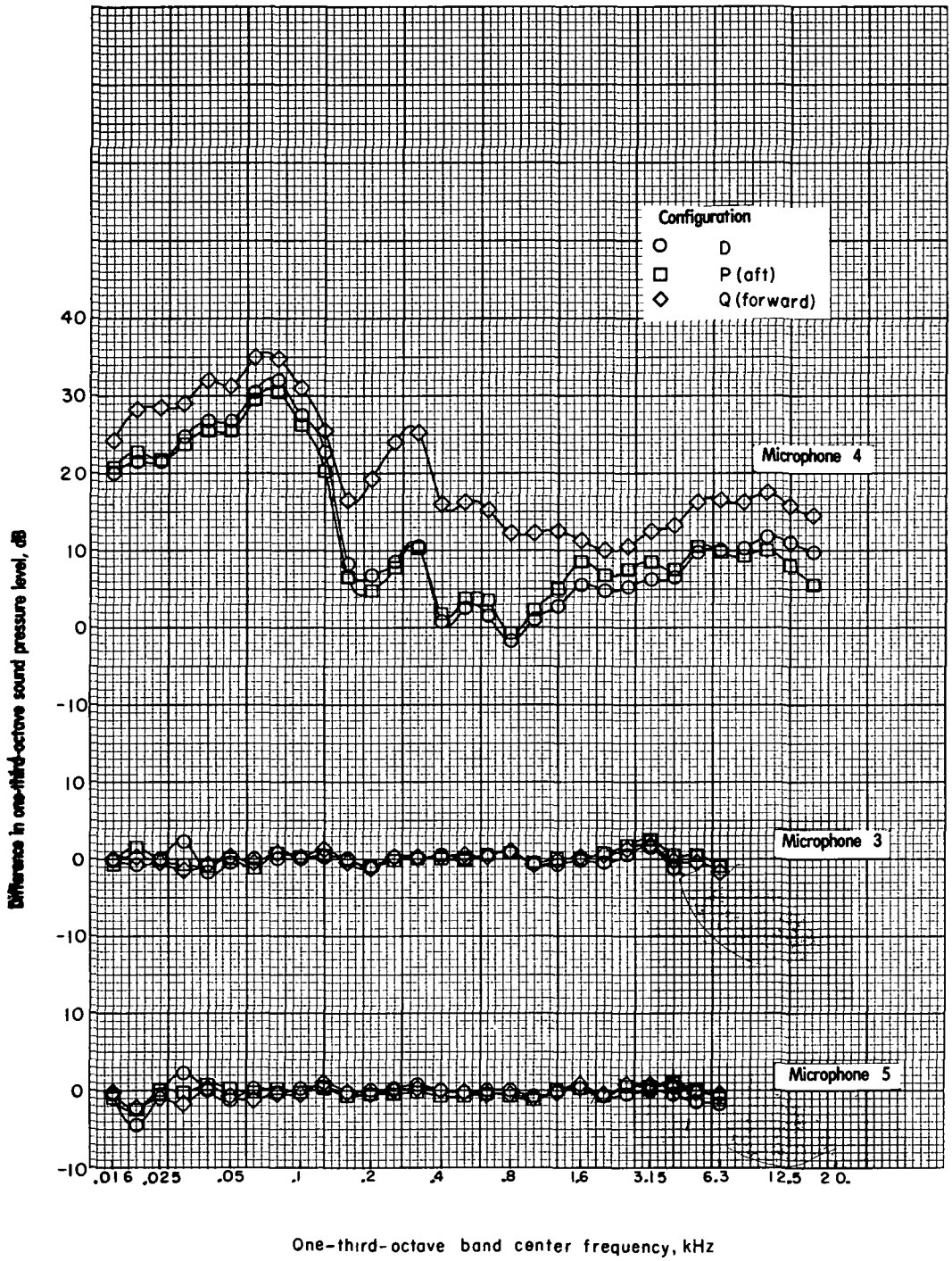

(a) 30.5 m/sec (100 ft/sec).

Figure 11.- Differences in one-third-octave sound pressure levels for different simulated landing-gear configurations and for two forward speeds.

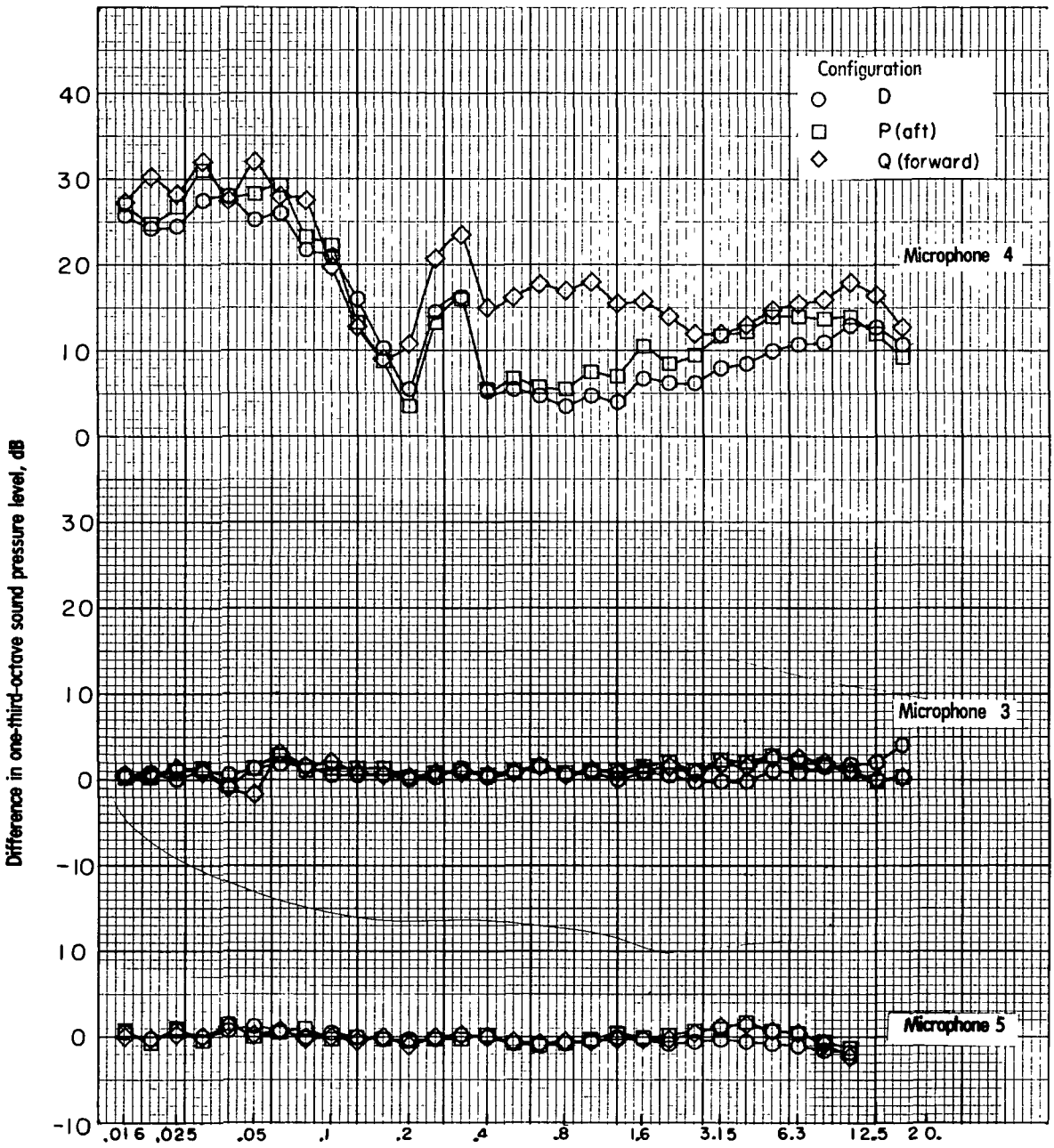

(b) 61.0 m/sec (200 ft/sec).

Figure 11.- Concluded.

1. Report No.	2 Government Accession No	3 Recipient's Catalog No
NASA TM-78658		

4 Title and Subtitle	5 Report Date
ACOUSTIC MEASUREMENTS OF A LARGE CAVITY IN A WIND TUNNEL	May 1978
	6 Performing Organization Code

7 Author(s)	8 Performing Organization Report No
James Scheiman	L-12022
	10 Work Unit No
	505-10-23-05

9 Performing Organization Name and Address	11 Contract or Grant No
NASA Langley Research Center Hampton, VA 23665	

12 Sponsoring Agency Name and Address	13 Type of Report and Period Covered
National Aeronautics and Space Administration Washington, DC 20546	Technical Memorandum
	14 Sponsoring Agency Code

15 Supplementary Notes

16 Abstract

Acoustic measurements of a large scale cavity have been made with inside and far-field microphones. Correlation of measured frequencies with available theories indicates that existing theories are applicable over a broader range than previously shown. The cavity configuration with a partial covering downstream seems to amplify the tonal intensities. The frequency of the tones seems to depend on cavity size, not on cavity open area. Introducing upstream disturbances seems to decrease the amplitude of the cavity tones.

17 Key Words (Suggested by Author(s))		18 Distribution Statement
Full scale	Acoustics	Unclassified - Unlimited
Cavity	Aircraft noise	
Airframe noise	Landing gear noise	Subject Category 71

19 Security Classif. (of this report)	20 Security Classif (of this page)	21 No of Pages	22 Price*
Unclassified	Unclassified	33	$4.50

* For sale by the National Technical Information Service, Springfield, Virginia 22161

NASA-Langley, 1978